

## Structures of Revertant Signal Sequences of *Escherichia coli* Ribose Binding Protein

Seung-Wook Chi,\* Gwan-Su Yi,<sup>§</sup> Jeong-Yong Suh,<sup>†</sup> Byong-Seok Choi,<sup>†</sup> and Hyoungman Kim\*

Departments of \*Biological Sciences and <sup>†</sup>Chemistry, Korea Advanced Institute of Science and Technology, Taejon 305-701, Korea, and <sup>§</sup>Magnetic Resonance Group, Korea Basic Science Center, Taejon 305-333, Korea

**ABSTRACT** Recently we reported (Yi et al., 1994) that the  $\alpha$ -helical content of the signal peptide of *Escherichia coli* ribose binding protein, when determined by circular dichroism (CD) and two-dimensional NMR in trifluoroethanol/water solvent, is higher than that of its nonfunctional mutant signal peptide. In the present investigation, the structures of the signal peptides of two revertant ribose binding proteins in the same solvent were also determined with CD and two-dimensional <sup>1</sup>H NMR spectroscopy. According to the CD results, both of these revertant signal peptides showed an intermediate helicity between those of wild-type and mutant signal peptides, the helical content of the revertant peptide with higher recovery of the translocation capability being higher. On the other hand, the  $\alpha$ -helix regions of the wild-type and the revertant peptides as determined by NMR were shown to be the same. This discrepancy may be due to the difference in stability between identical  $\alpha$ -helical stretches in wild-type and revertant peptides. A good correlation was observed between the helical content of these four ribose binding protein signal peptides in TFE/water as studied by CD and their in vivo translocation activities. It appears, therefore, that both the proper length of the helix and the stability are of functional significance.

### INTRODUCTION

Although translocation of newly synthesized proteins through the plasma membrane of *Escherichia coli* has been the subject of intensive studies (Wickner et al., 1991; Wolin, 1994; Tokuda, 1994), its mechanism is still poorly understood. Most of the secretory proteins exported from *E. coli* have signal sequences attached to the N-terminal end of the mature domains. Although the importance of the signal sequence for the translocation has been clearly established, its exact role has not yet been defined. It is thought that the signal peptides are involved in the targeting and modulation of the folding of the mature part. Also, because no homology of primary sequence of all known signal sequences has been found (von Heijne, 1985), the overall characteristics such as hydrophobicity and conformation have been proposed to be important in the translocation of the nascent protein (Gierasch, 1989).

Several studies of the conformations of isolated signal sequences suggested that the tendency of the sequences to assume  $\alpha$ -helical conformation is important to their functions. Gierasch and her co-workers investigated the structures of wild-type and various mutant signal sequences of LamB protein (Briggs, 1986; Bruch et al., 1989; McKnight et al., 1989; Bruch and Gierasch, 1990) and OmpA protein (Rizo et al., 1993). In all these peptides, the  $\alpha$ -helix was found to be the predominant structure in a 50% 2,2,2-trifluoroethanol(TFE)/water solution that mimics an amphiphilic environment. The results from combined circular

dichroism (CD) and two-dimensional (2D) NMR studies indicated that the stability of the  $\alpha$ -helical structure in a hydrophobic core is important.

In our previous investigation, the CD and 2D NMR experiments were carried out to elucidate the conformations of the wild-type signal sequences of the *E. coli* ribose binding protein (RBP; Met1-Asn2-Met3-Lys4-Lys5-Leu6-Ala7-Thr8-Leu9-Val10-Ser11-Ala12-Val13-Ala14-Leu15-Ser16-Ala17-Thr18-Val19-Ser20-Ala21-Asn22-Ala23-Met24-Ala25) and the signal sequence of a mutant (Yi et al., 1994). The mutant peptide (L9P) contains a Pro at position 9 instead of Leu as in the wild-type peptide. The precursor RBP with the mutant signal peptide does not show any translocation (Iida et al., 1985). The wild-type signal peptide was found to form an 18-residue-long  $\alpha$ -helix starting from the N-terminal region through the hydrophobic stretch in a solvent consisting of 10% dimethylsulfoxide, 40% water, and 50% TFE (by volume). The nonfunctional mutant peptide does not have any secondary structure in this solvent but forms a 12-residue-long  $\alpha$ -helix within the hydrophobic stretch in a TFE/water (50:50 by volume) solvent. Thus, it is apparent that the length of the  $\alpha$ -helix segment in the signal peptide is important for the translocation of the precursor RBP.

To obtain an additional correlation between the structure and translocation capability, we studied the structures of two revertant signal peptides that function as intragenic suppressors of the L9P mutant mentioned above with a second mutation within each signal sequence. One of them, first observed by Iida et al. (1985), has a double mutation (L9P, S11F) in the signal peptide, the mature domain being the same as that of the wild-type pRBP. Although the first mutation, L9P, abolishes the translocation, the second mutation, S11F, significantly recovers the translocation capability, as determined by pulse chase experiments (Teschke

Received for publication 24 April 1995 and in final form 31 August 1995.

Address reprint requests to Dr. Hyoungman Kim, Department of Biological Sciences, Korea Advanced Institute of Science and Technology, 373-1 Kusong-Dong, Yusong-Gu, Taejon 305-701, Korea. Tel.: 82-42-869-2602; Fax: 822-42-869-2610; E-mail: hmkim@sorak.kaist.ac.kr.

© 1995 by the Biophysical Society

0006-3495/95/12/2703/07 \$2.00

et al., 1991). The T8I mutation in another revertant signal peptide, in which the Thr at the position of 8 is replaced by an Ile, also overcomes the translocation deficiency brought about by the L9P mutation in the signal peptide, as judged from the swarm plate experiment (T. Song and C. Park, Korea Advanced Institute of Science and Technology, personal communication). No quantitative translocation experiments had been performed for the (L9P, T8I) revertant. In the present investigation, the structures of both of these signal peptides (L9P, S11F revertant peptide and L9P, T8I revertant peptide) in TFE/water were analyzed by CD and 2D NMR and compared with those of the wild-type and mutant signal peptides. The reason for choosing the TFE/water solvent for this study was discussed previously (Yi et al., 1994). Earlier, it was reported that the structure of peptides in a TFE/water solution is qualitatively similar to a membrane mimetic environment such as SDS micelles and phospholipid vesicles (Briggs, 1986; McKnight et al., 1989). Furthermore, this provides a simple system to compare critically the  $\alpha$ -helix-forming propensity of the four RBP signal peptides studied in this laboratory.

A quantitative translocation experiment for the (L9P, T8I) revertant was also performed so that the relationship between the secondary structure and the translocation capability for this mutant could be assessed.

## MATERIALS AND METHODS

### Synthesis and purification of signal peptides

Revertant signal peptides were synthesized by a solid phase method with a MilliGen 9060 automated peptide synthesizer. The peptides were purified by the reverse phase HPLC using a Phenomenex W-porex C<sub>8</sub> column (15 cm  $\times$  1.0 cm), elution being made with a water-acetonitrile linear gradient containing 0.1% trifluoroacetic acid. The sequences of the purified peptides were confirmed with a MilliGen/Biosearch 6600 prosequencer.

### Circular dichroism

The CD spectra were obtained on a Jasco J-600 spectropolarimeter using a 1-mm cell. The peptide concentration range used was 10  $\mu$ M–2 mM. The peptide concentration was determined by quantitative amino acid analysis. The temperature was maintained at either 25°C or 50°C by a NESLAB RTE-210 temperature controller. The mixed solvent used contained 50% (by volume) unbuffered water and 50% TFE (Sigma, St. Louis, MO), which is equivalent to 20 mol % TFE. Its pH was adjusted to 3.0 with 0.1-N HCl solution at room temperature. All CD spectra obtained were the average of seven consecutive scans from 250 to 200 nm and were baseline corrected and smoothed.

### Nuclear magnetic resonance spectroscopy

NMR spectra were obtained at 500 MHz on a Bruker AMX 500 spectrometer at 25°C and pH 3. The peptide concentrations used were 1.2 mM for the (L9P, S11F) revertant signal peptide and 2 mM for the (L9P, T8I) revertant signal peptide. Both peptides were dissolved in a mixed solvent of 50% trifluoroethanol-d<sub>3</sub> (Cambridge Isotope Laboratories, Andover, MA) and 50% unbuffered water (by volume).

Sequential assignments were obtained by total correlation spectroscopy (TOCSY) (Davis and Bax, 1985), double quantum filtered (DQF) correlation spectroscopy (COSY) (Rance et al., 1983), and two-dimensional

nuclear Overhauser effect spectroscopy (NOESY) (Macura et al., 1981). TOCSY results were collected with a mixing time of 75 ms. An MLEV-17 composite pulse (Bax and Davis, 1985) was used for the spin locking. To prevent phase distortion in the case of water suppression, the trim pulse was not used. The mixing time for the NOESY experiments was 240 ms. The water resonance was suppressed by preirradiation during the relaxation delay for TOCSY and DQF COSY. In the NOESY experiments, the HDO resonance was suppressed by irradiation during the relaxation delay and mixing period. The relaxation delay was 1.3 s in all experiments, and the carrier frequency was set on the HDO resonance. The 2D experiments were recorded with 512  $t_1$  measurements and 2048 data points in the  $t_2$  dimension. 88–352 transients were collected for each increment of  $t_1$  in the NOESY experiments, and 80 transients were acquired in the TOCSY experiments. The DQF COSY was recorded with 512  $t_1$  transients and 4096 data points in the  $t_2$  dimension to determine the  $J$ -coupling constants.

The 2D NMR data were processed with the Bruker program, UXNMR, on a Bruker X-32 workstation or with Felix 2.3 (Biosym Technologies, Inc., San Diego, CA) on an IRIS 4D-20 workstation (Silicon Graphics, Inc., Mountain View, CA). All 2D data sets were collected in the phase-sensitive mode by the time-proportional phase incrementation method (Marion and Wüthrich, 1983). The data were zero-filled to 1 K in the  $t_1$  dimension. Before Fourier transformation, a 60°-shifted squared sine bell function was multiplied to free induction decays in the NOESY, DQF COSY, and TOCSY experiments. A polynomial baseline correction was applied to the entire spectral range except for the water resonance region. The spectra were analyzed in both unsymmetrized and symmetrized forms, and the data sets presented are in unsymmetrized form.

### Determination of translocation rate by pulse labeling

The isolation of the revertant was carried out with the procedure described in the literature (Teschke et al., 1991). The AI287 (*rbsB::Tn10*) strain harboring plasmid pAI27, which carries the *rbsB103* mutation, was used to isolate the revertants that could suppress the export-defective signal sequence mutation, *rbsB103*. Two of the revertants have the mutational changes (L9P, S11F) and (L9P, T8I), respectively (Iida et al., 1985; T. Song and C. Park, Korea Advanced Institute of Science and Technology, personal communication).

Cells (strains used: CP627, CP631, TS23) were grown to a density of 10<sup>8</sup> cells/ml in a M9 minimal salts medium supplemented with 0.4% glycerol and 15- $\mu$ g/ml chloramphenicol at 35°C; vigorous shaking was applied. These cells were radiolabeled for 30 s by introduction of 30- $\mu$ Ci/ml [<sup>35</sup>S]methionine. Immediately afterward, an equal volume of non-radioactive 0.75% methionine was added. The time course of translocation was monitored by pipetting of 0.8 ml of the culture into 0.7 ml of 10% trichloroacetic acid. The samples were immunoprecipitated with an anti-serum to RBP, and the precipitates were analyzed by SDS-PAGE. The gels were dried and overlaid with an x-ray film, and the bands of RBP were quantified by densitometry.

## RESULTS

### Circular dichroism

Each of these two revertant signal peptides showed practically identical spectra at pH 3 and 7 (in 50% TFE and 50% 50 mM phosphate buffer by volume), suggesting that the conformation is not dependent on pH. No change in the CD spectra was observed when the concentration of these peptides was changed from 10  $\mu$ M to 2 mM, suggesting that no aggregation occurred in the concentration range studied. Fig. 1 presents the CD spectra of revertant signal peptides obtained at 25°C and 50°C. The CD spectra of the wild-type peptide and the mutant peptide previously obtained (Yi et

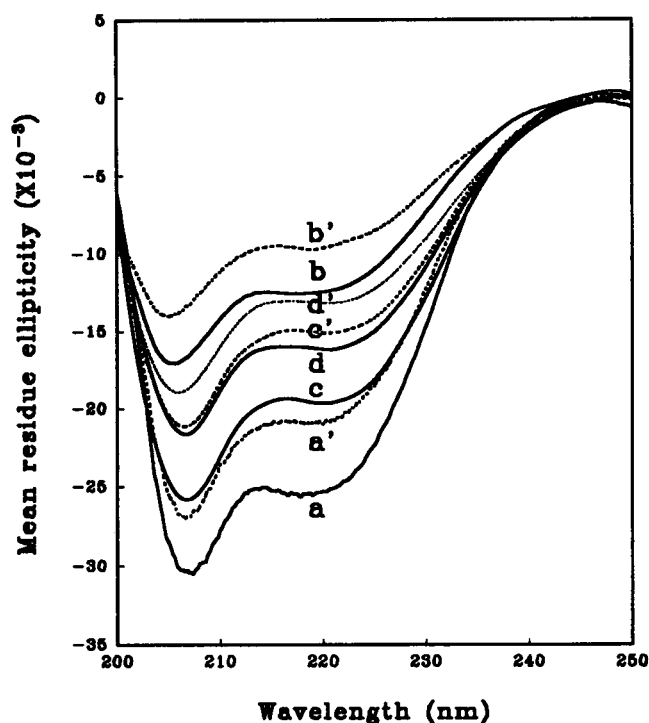


FIGURE 1 CD spectra of RBP signal peptides in a 20 mol % TFE/water solution at pH 3; (L9P, S11F) revertant at 25°C (c) and at 50°C (c'); (L9P, T8I) revertant at 25°C (d) and at 50°C (d'). The CD spectra of the wild-type peptide at 25°C (a) and at 50°C (a') and of the mutant peptide at 25°C (b) and at 50°C (b') in the same solvent (Yi et al., 1994) are also presented for comparison.

al., 1994) are also shown for comparison. All the CD spectra show minima at 206–208 nm with a shoulder near 222 nm, which is indicative of the presence of an  $\alpha$ -helical structure. The isodichroic point observed at 200–202 nm is consistent with a helix–random-coil interconversion. The CD spectra were curve-fitted by the least-squares method into the reference CD spectra of four conformations,  $\alpha$ -helix,  $\beta$ -sheet, turn, and random structure, based on five proteins, myoglobin, lactate dehydrogenase, lysozyme, papain, and ribonuclease (Yang et al., 1986). The estimated values of the  $\alpha$ -helix contents of wild-type, mutant, and revertant peptides are shown in Table 1. Although the  $\alpha$ -helical contents of these peptides decreased significantly with increasing temperature, the fractional decreases are similar.

TABLE 1  $\alpha$ -Helical contents of the RBP signal peptides obtained from CD spectra

| Signal Peptide        | $\alpha$ -Helix Contents* |             |
|-----------------------|---------------------------|-------------|
|                       | At 25°C (%)               | At 50°C (%) |
| Wild type             | 69                        | 56          |
| Mutant                | 33                        | 28          |
| (L9P, S11F) revertant | 57                        | 43          |
| (L9P, T8I) revertant  | 46                        | 35          |

\*Obtained by curve fitting to the reference spectra based on five proteins, myoglobin, lactate dehydrogenase, lysozyme, papain, and ribonuclease (Yang et al., 1986). The average error range was  $\pm 2\%$ .

## Resonance assignments

The  $^1\text{H}$  resonances in the NMR spectra of the (L9P, S11F) revertant peptide (Table 2) and the (L9P, T8I) revertant peptide (Table 3) were assigned by sequential assignment methodology (Billeter et al., 1982; Wüthrich, 1986). First, the complete spin system of amino acid residues was identified by use of the TOCSY spectra. Next, the sequential connectivities of the backbone protons were established by following the fingerprint region of the NOESY spectra (Fig. 2).

## Secondary structure of revertant signal peptides

The fingerprint region of the NOESY spectra of the revertant peptides in 50% TFE/water solution at 25°C is shown in Fig. 2. The NOESY spectra of the (L9P, S11F) revertant peptide at pH 3 and at pH 7 (not shown) were nearly identical. This agrees with the CD result, suggesting that the structures of these peptides at pH 3 and pH 7 are the same. The NOE crosspeaks in the NOESY spectra of these two revertant peptides are very similar. The NOESY spectra provide strong support for the presence of secondary structures in the peptide. A large number of crosspeaks connecting neighboring amide protons were observed from residues 3 to 20. Some  $\text{NH}(i)/\text{NH}(i+1)$  crosspeaks may have overlapped the diagonal line because the neighboring amide protons have very similar chemical shift values. The strong  $\text{NH}(i)/\text{NH}(i+1)$  connectivity of NOE crosspeaks is consistent with the presence of  $\alpha$ -helical segments in the peptide. The NH region of the NOESY spectra indicated that residues 3–20 of these peptides form  $\alpha$ -helical structures.

Medium-range  $\text{C}_\alpha\text{H}(i)/\text{NH}(i+3)$  interactions, which are also typical of a helical conformation, were clearly observed in residues 10–20 of these peptides, although some of them are apparently overlapped with other cross-peaks. The presence of these medium-range interactions in residues 3–9 was not apparent. The discrepancy between short-range interaction and medium-range interaction may simply reflect the difference in the conformational populations in different parts of the molecule. That is, the helical population of residues 3–9 is smaller than that of residues 10–20 because the helical structure is less stable in the N-terminal end than in the hydrophobic core region. The observed NMR parameters result from conformational averaging when more than one conformation interconverts. The average short-range  $\text{NH}(i)/\text{NH}(i+1)$  NOE interaction may be strong enough to be observed even in the N-terminal region, whereas the average medium range  $\text{C}_\alpha\text{H}(i)/\text{NH}(i+3)$  interaction in this region is too weak to be observed (Bruch et al., 1989). With a longer mixing time, such as 270 ms, some medium-range  $\text{C}_\alpha\text{H}(i)/\text{NH}(i+3)$  interactions can be seen: 3–6 in the (L9P, S11F) revertant peptide and 3–6 and 8–11 in the (L9P, T8I) revertant peptide. However, their intensities were much smaller than those of medium-range interactions in the hydrophobic core. The  $^3J_{\text{HN}\alpha}$  values estimated

**TABLE 2** Chemical shift values for (L9P, S11F) revertant signal peptide of *E. coli* RBP in TFE/water at 25°C\*

| Residue | NH   | $\alpha$ H | $\beta$ H  | $\gamma$ H | Others   |
|---------|------|------------|------------|------------|--|
| Met-1   |      |            |            |            |  |
| Asn-2   | 8.71 | 4.80       | 2.79, 2.90 |            | $\gamma$ NH <sub>2</sub> 6.73, 7.63  |
| Met-3   | 8.51 | 4.40       | 2.01, 2.13 | 2.57       | $\epsilon$ CH <sub>3</sub> 2.01  |
| Lys-4   | 8.10 | 4.15       | 1.69, 1.81 | 1.40       | $\delta$ CH <sub>2</sub> 1.78; $\epsilon$ CH <sub>2</sub> 2.99; $\epsilon$ NH <sub>3</sub> <sup>+</sup> 7.62 |
| Lys-5   | 7.82 | 4.16       | 1.70, 1.81 | 1.41       | $\delta$ CH <sub>2</sub> 1.78; $\epsilon$ CH <sub>2</sub> 2.98; $\epsilon$ NH <sub>3</sub> <sup>+</sup> 7.62 |
| Leu-6   | 7.61 | 4.28       | 1.66       | 1.59       | $\delta$ CH <sub>3</sub> 0.72  |
| Ala-7   | 7.76 | 4.34       | 1.39       |            |  |
| Thr-8   | 7.67 | 4.47       | 4.25       | 1.23, 1.40 |  |
| Pro-9   |      | 4.41       | 2.00, 2.27 | 2.00       | $\delta$ CH <sub>3</sub> 3.81  |
| Val-10  | 7.43 | 3.74       | 2.03       | 0.89, 0.97 |  |
| Phe-11  | 7.55 | 4.32       | 3.15       |            | Ring 2,6H 7.18, 4H 7.24, 3,5H 7.27   |
| Ala-12  | 7.74 | 4.00       | 1.45       |            |  |
| Val-13  | 7.73 | 3.58       | 2.17       | 0.89, 1.01 |  |
| Ala-14  | 8.03 | 4.03       | 1.42       |            |  |
| Leu-15  | 8.57 | 4.03       | 1.59       | 1.43       | $\delta$ CH <sub>3</sub> 0.83  |
| Ser-16  | 7.98 | 4.10       | 3.95, 4.03 |            |  |
| Ala-17  | 8.48 | 4.12       | 1.49       |            |  |
| Thr-18  | 7.93 | 3.99       | 4.39       | 1.23       |  |
| Val-19  | 8.40 | 3.79       | 2.14       | 0.93, 1.02 |  |
| Ser-20  | 8.00 | 4.24       | 3.92, 4.00 |            |  |
| Ala-21  | 7.92 | 4.21       | 1.48       |            |  |
| Asn-22  | 7.93 | 4.61       | 2.80       |            | $\gamma$ NH <sub>2</sub> 6.71, 7.57  |
| Ala-23  | 8.01 | 4.29       | 1.46       |            |  |
| Met-24  | 7.84 | 4.47       | 2.04, 2.16 | 2.55       | $\epsilon$ CH <sub>3</sub> 2.04  |
| Ala-25  |      |            |            |            |  |

\*Chemical shifts are in ppm relative to 3.88 ppm for trifluoroethanol methylene resonance. The estimated error is  $\pm 0.02$  ppm.

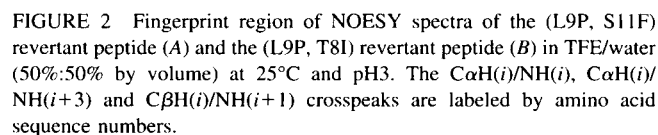
from the DQF COSY spectrum were found to be less than 6 Hz for the residues from 3 to 20 for both revertant peptides, which supports the notion that these polypeptide chains are mostly in the form of an  $\alpha$  helix. Only a few

NH(*i*)/NH(*i*+2) and C $\alpha$ H(*i*)/NH(*i*+4) interactions were observed. It is usually difficult to observe NOEs between protons more than 3.5 Å apart in small peptides having fewer than 30 residues because of the short correlation time

**TABLE 3** Chemical shift values for (L9P, T8I) revertant signal peptide of *E. coli* RBP in TFE/water at 25°C

| Residue | NH   | $\alpha$ H | $\beta$ H  | $\gamma$ H | Others   |
|---------|------|------------|------------|------------|--|
| Met-1   |      |            |            |            |  |
| Asn-2   | 8.71 | 4.80       | 2.79, 2.90 |            | $\gamma$ NH <sub>2</sub> 6.76, 7.63  |
| Met-3   | 8.51 | 4.42       | 1.98, 2.12 | 2.55       | $\epsilon$ CH <sub>3</sub> 1.98  |
| Lys-4   | 8.10 | 4.16       | 1.68, 1.80 | 1.38       | $\delta$ CH <sub>2</sub> 1.50; $\epsilon$ CH <sub>2</sub> 2.98; $\epsilon$ NH <sub>3</sub> <sup>+</sup> 7.60 |
| Lys-5   | 7.80 | 4.17       | 1.75, 1.83 | 1.37       | $\delta$ CH <sub>2</sub> 1.48; $\epsilon$ CH <sub>2</sub> 2.97; $\epsilon$ NH <sub>3</sub> <sup>+</sup> 7.60 |
| Leu-6   | 7.63 | 4.20       | 1.64       | 1.61       | $\delta$ CH <sub>3</sub> 0.84, 0.88  |
| Ala-7   | 7.79 | 4.27       | 1.36       |            |  |
| Ile-8   | 7.62 | 4.30       | 1.87       | 1.13, 1.48 | $\gamma$ CH <sub>3</sub> 0.91, $\delta$ CH <sub>3</sub> 0.84   |
| Pro-9   |      | 4.47       | 1.99, 2.21 | 1.99       | $\delta$ CH <sub>2</sub> 3.67, 3.76  |
| Val-10  | 7.73 | 3.79       | 2.05       | 0.93, 1.00 |  |
| Ser-11  | 7.91 | 4.19       | 3.89, 3.98 |            |  |
| Ala-12  | 7.86 | 4.17       | 1.46       |            |  |
| Val-13  | 7.69 | 3.59       | 2.15       | 0.90, 0.99 |  |
| Ala-14  | 8.05 | 4.05       | 1.43       |            |  |
| Leu-15  | 8.28 | 4.12       | 1.73       | 1.64       | $\delta$ CH <sub>3</sub> 0.86  |
| Ser-16  | 8.04 | 4.11       | 3.95, 4.05 |            |  |
| Ala-17  | 8.45 | 4.11       | 1.48       |            |  |
| Thr-18  | 7.91 | 3.98       | 4.39       | 1.22       |  |
| Val-19  | 8.35 | 3.78       | 2.13       | 0.92, 1.02 |  |
| Ser-20  | 8.00 | 4.11       | 3.89, 3.98 |            |  |
| Ala-21  | 7.91 | 4.19       | 1.47       |            |  |
| Asn-22  | 7.87 | 4.59       | 2.78       |            | $\gamma$ NH <sub>2</sub> 6.70, 7.54  |
| Ala-23  | 7.99 | 4.23       | 1.44       |            |  |
| Met-24  | 7.81 | 4.44       | 2.04, 2.14 | 2.55, 2.64 | $\epsilon$ CH <sub>3</sub> 2.04  |
| Ala-25  | 7.73 | 4.30       | 1.42       |            |  |

\*Chemical shifts are in ppm relative to 3.88 ppm for trifluoroethanol methylene resonance. The estimated error is  $\pm 0.02$  ppm.



There are NOE connectivities between  $\delta\text{CH}$  of the Pro and NH of the preceding residue in both revertant peptides (Fig. 2), suggesting that the Pro residues are involved in the

Schematic diagrams summarizing the various connectivities observed in the NOESY spectra of wild-type, mutant, and two revertant peptides are shown in Fig. 3.

The time course of the processing of (L9P, T8I) revertant pRBP, as studied by the pulse-labeling experiment, was similar to that of (L9P, S11F) revertant pRBP (Teschke et al., 1991) and reaches the saturation point in less than 2 min. The efficiency of translocation is defined as the fraction of the precursor RBP processed into the mature RBP. These values were corrected to compensate for the distribution of methionine. The translocation efficiency of (L9P, T8I) revertant RBP was found to be 83%. The value for (L9P, S11F) revertant RBP was shown to be 93% (Teschke et al., 1991).

The primary aim of this investigation was to determine the correlation between the  $\alpha$ -helix-forming propensity of the several signal peptides and the translocation efficiency of the corresponding precursor RBP. The CD results have shown that the helical contents of the revertant peptides are intermediate between those of the wild-type (69%) and the nonfunctional mutant peptides (33%). This result and the observation that the  $\alpha$ -helical content of the (L9P, S11F) revertant peptide (57%) is higher than that of the (L9P, T8I) revertant peptide (46%) suggest that the overall  $\alpha$ -helical content is important for the function of signal peptides.

The  $\alpha$ -helical content values obtained by CD experiments may reflect both the length of the  $\alpha$ -helix stretch and the stability of the stretch. For the case of the mutant peptide, the NMR results agree with the CD results, indicating that it has a shorter  $\alpha$ -helical segment than the wild-type peptide (Yi et al., 1994). However, the NMR results in this investigation also showed that both of the revertant peptides have  $\alpha$ -helical stretches identical to those of the wild-type peptide, from residues 3 to 20. This apparent discrepancy in the results of CD and NMR experiments may simply mean that the wild-type peptide has a higher population of  $\alpha$ -helix in this region than the (L9P, S11F) peptide, whereas the  $\alpha$ -he-

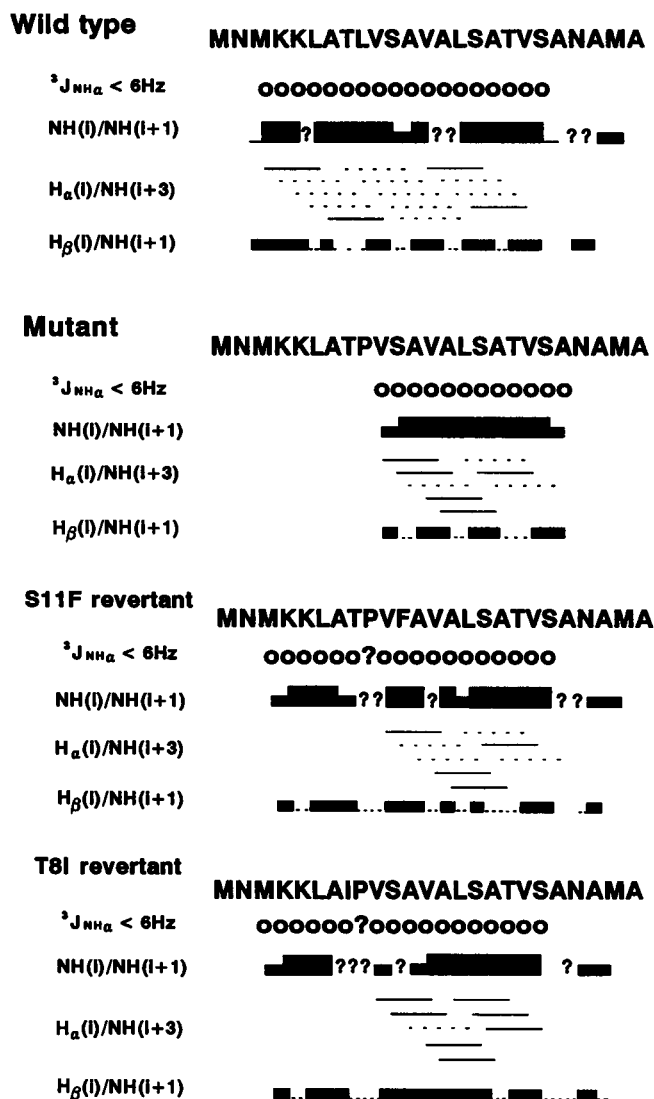


FIGURE 3 Schematic representation of the summary of NMR data. The residues that have  $^3J_{NH\alpha}$  values of less than 6 Hz are represented by open circles. The thicknesses of the lines represent the intensity of NOE, and the question marks indicate the crosspeaks that are indistinguishable because of their proximity to the diagonal. The dashed lines in the medium-range NOEs are the crosspeaks overlapped by other crosspeaks such as intrareidue crosspeaks. Diagrams for the wild-type and the mutant type peptides given in a previous publication (Yi et al., 1994) are also shown for comparison.

lix population of (L9P, T8I) peptide is even smaller. This is corroborated by the observation that, unlike in the wild-type peptide, the medium range NOE interaction is absent in the N-terminal region of the revertant peptides. This indicates that the stability of the  $\alpha$ -helical segment, which is reflected on the  $\alpha$ -helical population, is also important for the function of the signal peptide. On the other hand, the mutant peptide, with the shortest  $\alpha$ -helical stretch, has no translocation capability. It is possible that both the critical length of the  $\alpha$ -helical segment and its stability are essential for the function. The fact that a second mutation, which overcomes the shortening of the  $\alpha$ -helical segment by the first muta-

tion, largely recovers the translocation capability again suggests the importance of the length and the stability of the  $\alpha$ -helical segment.

A similar conclusion was drawn by Gierasch and her co-workers in connection with the signal peptides of wild-type LamB and its mutants (Bruch and Gierasch, 1990). Although the lengths of the  $\alpha$ -helical segments of wild-type LamB and RBP in TFE/water solution are similar, the locations of these segments within the signal peptides are different. This suggests that the general requirements for the function of a signal peptide may not be the location of the helix but rather the proper length and stability of the helix. The common requirement of an  $\alpha$ -helix stretch of proper length and stability in these diverse precursor proteins is of considerable interest because targeting mechanisms of precursor proteins may be different. For example, LamB is translocated through the SecB/SecA pathway posttranslationally, whereas RBP is, at least in part, cotranslationally translocated via the Ffh/SecA route (Wolin, 1994). It may be that the  $\alpha$ -helical structure of the signal peptides is important when the peptides form complexes with SecA and/or either one of the chaperone proteins. The proper length of helix is thought to be that required to span the membrane directly or to occupy the binding site of the protein components of translocation machinery (Bruch and Gierasch, 1990).

It must be stressed that the present work merely correlates the  $\alpha$ -helix contents of RBP signal peptides in the artificial environment of a TFE/water solution with the translocation capabilities of corresponding precursor RBPs. Although the propensity for  $\alpha$ -helix formation by signal peptides appears to be important for the translocation, the real biological significance of the present observation is unclear, primarily because the detailed mode of interaction between the signal peptide and the translocation machinery of *E. coli* is unknown. For many of the *E. coli* proteins that are secreted into the periplasmic space the initial interaction of targeting is with SecB, but pRBP is apparently independent of this chaperone. Recently it was shown that the Ffh protein, which is analogous to the 54-kDa subunit of the mammalian signal-recognition particle, is at least partly involved in the RBP targeting. Ffh has several Met-rich patches of some 25 amino acid residues that may form amphiphilic  $\alpha$ -helical structures. It was proposed that these patches form a hydrophobic groove with flexible hydrophobic Met residues accommodating the signal peptides of a variety of amino acid sequences (Bernstein et al., 1989). It is possible that the environment of TFE/water may be akin to that of the groove lined with Met and other hydrophobic side chains.

Another interesting feature of our results is the change in the length of the  $\alpha$ -helical segment brought about by the amino acid substitution. The length of an  $\alpha$ -helical structure in proteins is thought to depend on the interaction of the helix-end residues with the side-chain groups of the neighboring residues (Presta and Rose, 1988; Richardson and Richardson, 1988). Of particular interest here is how the amino acid substitutions on both sides of the Pro9 of the

mutant peptide bring about the extension of the  $\alpha$ -helical segments toward the N-terminal end of the peptide beyond Pro9. This is an important and interesting problem to be addressed.

We thank Professor Chankyu Park and Dr. Taeksun Song for helpful comments and for the isolation of the revertant and Dr. Myeong-Jun Choi for the peptide synthesis. This study was supported in part by the Korea Science and Engineering Foundation and also by the Korea Research Center for Theoretical Physics and Chemistry.

## REFERENCES

- Bax, A., and D. G. Davis. 1985. MLEV-17-based two-dimensional homonuclear magnetization transfer spectroscopy. *J. Magn. Reson.* 65: 355–360.
- Bazzo, R., M. J. Tappin, A. Pastore, T. S. Harvey, J. A. Carver, and I. D. Campbell. 1988. The structure of melittin. A  $^1\text{H}$ -NMR study in methanol. *Eur. J. Biochem.* 173:139–146.
- Bernstein, H. D., M. A. Poritz, K. Strub, P. J. Hoben, S. Brenner, and P. Walter. 1989. Model for signal sequence recognition from amino-acid sequence of 54K subunit of signal recognition particle. *Nature (London)*. 340:482–486.
- Billeter, M., W. Braun, and K. Wüthrich. 1982. Sequential resonance assignments in protein  $^1\text{H}$  nuclear magnetic resonance spectra. *J. Mol. Biol.* 155:321–346.
- Briggs, M. S. 1986. Biophysical studies of signal sequences. Ph.D. dissertation. Yale University.
- Bruch, M. D., and L. M. Gierasch. 1990. Comparison of helix stability in wild-type and mutant LamB signal sequences. *J. Biol. Chem.* 265: 3851–3858.
- Bruch, M. D., C. J. McKnight, and L. M. Gierasch. 1989. Helix formation and stability in a signal sequence. *Biochemistry*. 28:8554–8561.
- Davis, D. G., and A. Bax. 1985. Assignment of complex  $^1\text{H}$  NMR spectra via two-dimensional homonuclear Hartman–Hahn spectroscopy. *J. Am. Chem. Soc.* 107:2820–2821.
- Gierasch, L. M. 1989. Signal sequence. *Biochemistry*. 28:923–930.
- Iida, A., J. M. Groarke, S. Park, J. Thom, H. Zabicky, G. L. Hazelbauer, and L. L. Randall. 1985. A signal sequence mutant defective in export of ribose-binding protein and a corresponding pseudorevertant isolated without imposed selection. *EMBO J.* 4:1875–1880.
- Inagaki, F., I. Shimada, K. Kawaguchi, M. Hirano, I. Terasawa, T. Ikura, and N. Go. 1989. Structure of melittin bound to perdeuterated dodecylphosphocholine micelles as studied by two-dimensional NMR and distance geometry calculations. *Biochemistry*. 28:5985–5991.
- Macura, S., Y. Huang, D. Suter, and R. R. Ernst. 1981. Two-dimensional chemical exchange and cross-relaxation spectroscopy of coupled nuclear spins. *J. Magn. Reson.* 43:259–281.
- McKnight, C. J., M. S. Briggs, and L. M. Gierasch. 1989. Functional and nonfunctional LamB signal sequence can be distinguished by their biophysical properties. *J. Biol. Chem.* 264:17293–17297.
- Marion, D., and K. Wüthrich. 1983. Application of phase sensitive two-dimensional correlated spectroscopy (COSY) for measurements of  $^1\text{H}$ - $^1\text{H}$  spin-spin coupling constants in proteins. *Biochem. Biophys. Res. Commun.* 113:967–974.
- Presta, L. G., and G. D. Rose. 1988. Helix signals in proteins. *Science*. 240:1632–1641.
- Rance, M., O. M. Sørensen, G. Bodenhausen, G. Wagner, R. R. Ernst, and K. Wüthrich. 1983. Improved spectral resolution in COSY  $^1\text{H}$  NMR spectra of protein via double quantum filtering. *Biochem. Biophys. Res. Commun.* 117:479–485.
- Richardson, J. S., and D. C. Richardson. 1988. Amino acid preferences for specific locations at the ends of  $\alpha$  helices. *Science*. 240:1648–1652.
- Rizo, J., F. J. Blanco, B. Kobe, M. D. Bruch, and L. M. Gierasch. 1993. Conformational behavior of *Escherichia coli* OmpA signal peptides in membrane mimetic environments. *Biochemistry*. 32:4881–4894.
- Teschke, C. M., J. Kim, T. Song, S. Park, C. Park, and L. L. Randall. 1991. Mutations that affect the folding of ribose-binding protein selected as suppressors of a defect in export in *Escherichia coli*. *J. Biol. Chem.* 266:11789–11796.
- Tokuda, H. 1994. Biochemical characterization of the presecretory protein translocation machinery of *Escherichia coli*. *FEBS Lett.* 346:65–68.
- von Heijne, G. 1985. Signal sequences the limits of variation. *J. Mol. Biol.* 184:99–105.
- von Heijne, G. 1991. Proline kinks in transmembrane  $\alpha$ -helices. *J. Mol. Biol.* 218:499–503.
- Wickner, W., A. J. M. Driessen, and F. Hartl. 1991. The enzymology of protein translocation across the *Escherichia coli* plasma membrane. *Annu. Rev. Biochem.* 60:101–124.
- Williams, K. A., and C. M. Deber. 1991. Proline residues in transmembrane helices: structural or dynamic role? *Biochemistry*. 30:8919–8923.
- Wolin, S. L. 1994. From the elephant to E.coli: SRP-dependent protein targeting. *Cell*. 77:787–790.
- Woelfson, D. N., and D. H. Williams. 1990. The influence of proline residues on  $\alpha$ -helical structure. *FEBS Lett.* 277:185–188.
- Wüthrich, K. 1986. NMR of Proteins and Nucleic Acids. John Wiley & Sons, New York. 292 pp.
- Yamamoto, Y., T. Ohkubo, A. Kohara, T. Tanaka, T. Tanaka, and M. Kikuchi. 1990. Conformational requirement of signal sequence functioning in yeast: circular dichroism and  $^1\text{H}$  nuclear magnetic resonance studies of synthetic peptides. *Biochemistry*. 29:8998–9006.
- Yang, J. T., C.-S. C. Wu, and H. M. Martinez. 1986. Calculation of protein conformation from circular dichroism. *Methods Enzymol.* 130:208–269.
- Yi, G., B. Choi, and H. Kim. 1994. Structures of wild-type and mutant signal sequences of *Escherichia coli* ribose binding protein. *Biophys. J.* 66:1604–1611.